Solubility of Tridodecylamine in Supercritical Carbon Dioxide

Mohammad Kaboudvand and Hassan S. Ghaziaskar*

Department of Chemistry, Isfahan University of Technology, Isfahan, 84156-83111, I.R. Iran

Using a continuous flow apparatus, the solubility of tridodecylamine (TDA) in supercritical CO_2 ($scCO_2$) has been measured at temperatures of (308.1, 318.1, and 328.1) K in the pressure range of (8.0 to 40.0) MPa and a flow rate of (150 ± 10) mL·min^{-1}. At (308.1 and 318.1) K, the solubility increases with pressure up to 15.0 MPa where it reaches a plateau. At 328.1 K, the solubility increases with pressure up to 35.0 MPa, and then a plateau is observed. The solubility data were correlated using the Bartle equation and the Mendez−Santiago and Teja model. The Mendez−Santiago and Teja model correlated the solubility data better than the Bartle equation. TDA may be considered as a highly soluble compound in $scCO_2$.

Introduction

In recent years, many supercritical fluids (SCFs) have been used as useful solvents in many applications, such as in polymer,[1,2] food,[3] and pharmaceutical processing,[4] performing chemical reactions,[5] and separations.[6] Among different SCFs, $scCO_2$ has been widely used because it is nonflammable, nontoxic, inexpensive, and environmentally safe and it has low critical temperature and pressure. Recently, $scCO_2$ modified by suitable chelating agents has been used to develop new techniques for the extraction of transition metal ions from various solid and liquid matrices.[7,8]

The solubility data of solids and liquids in SCFs are very important in developing any supercritical extraction process. Solubilities of numerous solutes in a number of SCFs are now available in the literature,[9,10] and several methods have been developed to correlate and extrapolate the solubility data at various pressures and temperatures. Some of these correlation methods are highly empirical, while others are based on fundamental equations of state.[11,12]

Reactivity of CO_2 is generally low, but it does react with primary and secondary amines at low temperatures and pressures to form carbamates. The chemistry between CO_2 and amines is simply acid−base equilibrium.[13,14] Studies of amine−CO_2 reactions are mostly performed in aqueous systems, and this kind of information in organic solvents and especially in $scCO_2$ is hardly available.[15,16] On the other hand, aliphatic tertiary amines dissolved in an organic solvent are powerful extractants for carboxylic acids and can be used in reactive extraction processes for recovery of solutes like phenol, aniline, and some carboxylic acids.[17] For example, tridodecylamine (TDA) was used as the extractant for the recovery of shikmic and quinic acids.[18]

Tertiary amines with long hydrocarbon chains, such as trioctylamine (TOA) and TDA, have been used in the extraction of metals such as platinum and ruthenium.[19] A variety of organic chelating agents, such as crown ethers, dithiocarbamates, β-diketones, and tributylphosphates have been used for the extraction of metal ions from various solvents by using supercritical solvents.[20–22]

* Corresponding author. E-mail: ghazi@cc.iut.ac.ir. Tel.: 0098-311-3913260. Fax: 0098-311-3912350.

The motivation for this work stems from our interest in the chemical separation of dicarboxylic acids and precious metals using $scCO_2$. SCFs have been used as an environmentally friendly solvent to perform chemical reaction and separations. The most attractive features of this new technology include high solubilities of chelating agents and resultant metal complexes in $scCO_2$ and selectivity of the chelating agents. Since tertiary amines are not reacted with $scCO_2$, its solubility can be measured to evaluate its applicability for the reactive chemical separation using $scCO_2$. To the best of our knowledge, the solubility of TDA in $scCO_2$ has not been previously reported. Therefore, the solubility of TDA was measured at different pressures and temperatures to evaluate the applicability of TDA for chemical separation of dicarboxylic acids and precious metals using $scCO_2$. The research is in progress in our laboratory to use tertiary amines for the extraction of carboxylic acids and metals from aqueous media using ion-pair formation and $scCO_2$ as a green solvent.

Experimental

Materials. TDA with purity >95 % was purchased from Merck Co. The purity of CO_2 was more than 99.95 mass %, and it was purchased from Zam Zam Co. (Isfahan, Iran). All of the chemical reagents were used without any further purification.

Apparatus and Procedure. The solubility measurements were carried out using a continuous flow apparatus reported elsewhere[23] and shown in Figure 1. The apparatus mainly consists of a CO_2 cylinder, a HPLC pump (model LC-6A, Shimadzu Co.), two cells in series, an oven (model CO-2060 plus, JASCO, Japan) with the ability to set its temperature within ± 0.1 K, a back-pressure regulator (BPR) (model BP 1580-81, JASCO, Japan), a solute collector, a wet gas meter (model W-NK-1B, Shinagawa Crop., Japan), valves, and fittings of various types.

In each experiment (2.0 ± 0.1) mL of TDA was placed in the equilibrium cell, which was filled with Pyrex wool. Liquid carbon dioxide was directed into the cooled pump head and was pressurized through a preheated coil in the oven and enabled CO_2 to reach the oven temperature before it entered the cell. At the beginning of each experiment, the system was kept at the desired temperature and pressure for 45 min (i.e., static condition) to reach equilibrium.

After that, at a constant and low flow rate, to ensure that all experiments are carried out at the equilibrium and saturation

10.1021/je8001656 CCC: $40.75
Published on Web 06/28/2008

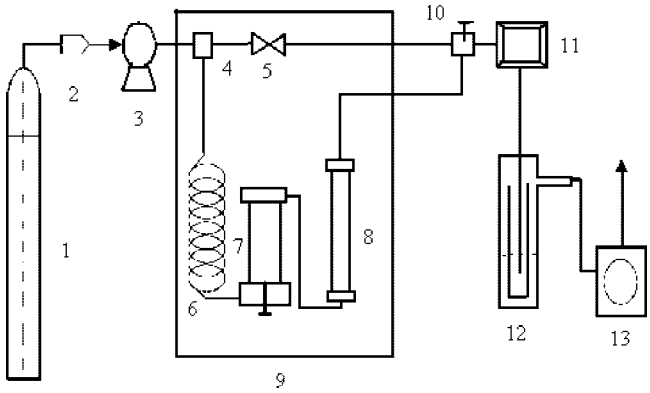

Figure 1. Schematic of the experimental apparatus used for measurement of the solubility in the supercritical fluid. 1, CO_2 cylinder; 2, chiller; 3, HPLC pump; 4, three-way connector; 5, needle valve; 6, preheating coil; 7, a three-port equilibrium vessel; 8, a two-port equilibrium cell; 9, oven; 10, three-way needle valve; 11, back pressure regulator; 12, collection tube; 13, wet gas meter.

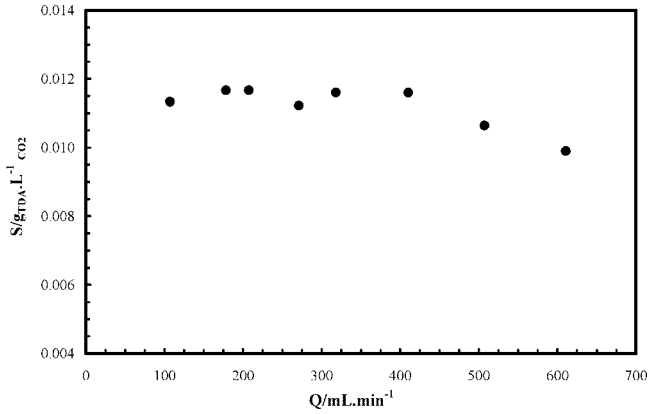

Figure 2. Solubility of TDA ($g_{TDA}\cdot L^{-1}_{CO2}$) vs expanded CO_2 flow rate (Q) at a pressure of 22.0 MPa and temperature of 318.1 K.

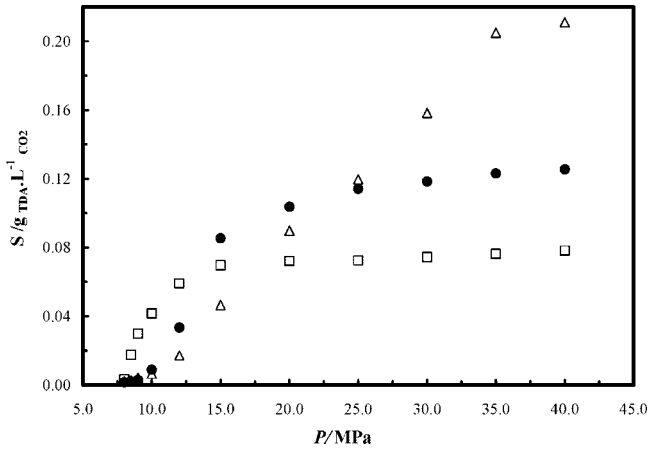

Figure 3. Solubility of TDA ($g_{TDA}\cdot L^{-1}_{CO2}$) in the pressure range of (8.0 to 40.0) MPa at temperatures □, 308.1 K; ●, 318.1 K; and Δ, 328.1 K.

conditions, the saturated $scCO_2$ was depressurized via a BPR. Using the constant flow rate mode of the piston pump, constant pressure (± 0.1 MPa) was maintained by the BPR. The volume of CO_2 was determined using a wet gas meter.

To ensure that saturation and equilibrium condition had been reached, the solubility of TDA was measured at 318.1 K and 22.0 MPa at various flow rates of CO_2 expanded gas (Q) from (80 to 610) $mL\cdot min^{-1}$ as shown in Figure 2. Since constant solubilities (i.e., (0.1150 ± 0.0028) $g_{TDA}\cdot L^{-1}_{CO2}$) were observed, it was concluded that the saturation and equilibrium condition had been reached. Therefore, the flow rate of (150 ± 10) $mL\cdot min^{-1}$ was selected for the other measurements.

For binary solubility measurements, the dissolved solutes after exiting from the BPR were trapped and collected in a vial filled with Pyrex wool. Finally, the trapped solute was weighed with an analytical balance (± 0.1 mg). On the basis of measured solute mass and solvent volume, the solubility in terms of $g\cdot L^{-1}$ and mole fraction were obtained. Having the time of sample collection and the volume of CO_2 passed through the wet gas meter, the expanded gas flow rate was calculated. Different volumes of CO_2 gas were collected for solubility measurements ranging from (200 to 500) mL at high (>12.0 MPa) and low pressures (<12.0 MPa), respectively. Each reported datum is an average of at least three and a maximum of four replicate experiments. The percent relative standard deviations of the measurements (% RSD) were generally less than 13 %.

Notice: At the time of the system adjustment, the exiting material from the BPR was entered into a solution of concentrated H_2SO_4 to trap the exiting amine−CO_2 aerosol.

Results and discussion

The solubility data of TDA in $scCO_2$ at different temperatures of (308.1, 318.1, and 328.1) K in the pressure range of (8.0 to 40.0) MPa were measured, as shown in Table 1 and Figure 3. The solubility of TDA in $scCO_2$ was calculated as mole fraction (y_2) and g_{TDA} per L of expanded CO_2 gas (S). The experimental results were correlated using the Bartle[24] and Mendez−Santiago and Teja[25] equations.

Effect of Pressure on the Solubility of TDA in scCO₂. The solubility of TDA in $scCO_2$ increases with pressure while showing different trends at different temperatures. At (308.1 and 318.1) K, the solubility increases with pressure up to 15.0 MPa where it reaches a plateau. At 328.1 K, the solubility increases with pressure up to 35.0 MPa, and then a plateau is observed.

The solubility in $scCO_2$ is strongly influenced by the system pressure, which determines the density of the $scCO_2$ as a solvent.[26] Crossover points in Figure 3 are observed for the different isotherms at about (14, 18, and 24) MPa. At the pressures less than the crossover points, the solute is more soluble at the lower temperatures, but at the pressures higher than the crossover points, the solute is more soluble at the higher temperatures. The crossover point is a consequence of competition between the $scCO_2$ density and TDA vapor pressure. At the pressures lower than the crossover pressure, the density effect is dominant, leading to the decrease of the solubility of the solute as a function of temperature. At the pressures higher than the crossover pressure, the density of the solvent becomes less effective, and the vapor pressure plays a major role in increasing the solubility. The solubility of TDA increases with increasing pressure at constant temperature. Influence of pressure on the solubility is more significant at higher temperatures because of the effect of vapor pressure. Therefore, the solubility of TDA in $scCO_2$ increases with pressure.

Effect of Temperature on the Solubility of TDA in scCO₂. Temperature affects the solubility in two opposite ways: the density of the fluid decreases with increasing temperature, which leads to the lower solubility at the higher temperatures, while the volatility of the solute increases with temperature and an increase in the solubility is observed at the higher temperatures. The density effect is dominant at the lower temperatures, and the solubility increases at the lower temperatures. At the higher pressures, the density of CO_2 is not as sensitive to the pressure as it is at the lower pressures. The volatility effect

becomes dominant, and the solubility increases at the higher temperatures. The solubility trend at 328.1 K is different and increased with pressure until 35.0 MPa.

Data Correlation. The experimental results from the present study were correlated by the two different density-based correlation models proposed by Bartle and Mendez−Santiago and Teja. The Bartle equation is given as

$$\ln\left(\frac{y_2 \cdot p}{p_{\text{ref}}}\right) = A + C(\rho_1 - \rho_{\text{ref}}) \quad (1)$$

where A is given by eq 2; y_2 is the mole fraction solubility; p is the system pressure (MPa); A and C are constants; P_{ref} is the standard pressure (i.e., 0.1 MPa); ρ_1 is the density of $scCO_2$; and ρ_{ref} is the reference density for which a value of 700 $kg \cdot m^{-3}$ was used for calculations.

$$A = a + \left(\frac{b}{T}\right) \quad (2)$$

The reason for using ρ_{ref} is to make the value of A much less sensitive to the data experimental error and to avoid the large variations caused by extrapolation to zero density.[27] TDA experimental solubility data were fitted by eq 1, i.e., the $\ln(y_2 \cdot P/P_{\text{ref}})$ values versus ρ_1 for the pressure range studied (Figure 4). The value of C, i.e., the slope of the line fitted into the data, is constant over the temperature range of (308.1 to 328.1) K as shown in Figure 4. The error of the experimentally measured solubility and the solubility given by the Bartle equation were estimated by calculating the average absolute relative deviation (AARD) between the experimental and the calculated solubility data using the following equation, where n is the number of solubility experimental data.

$$\text{AARD}\ (\%) = \frac{1}{n}\Sigma\left|\frac{y_{2(\text{exptl})} - y_{2(\text{calcd})}}{y_{2(\text{exptl})}}\right| \cdot 100 \quad (3)$$

Finally, the Mendez−Santiago and Teja model that is based on the simple theory of dilute solutions was used.[25] According to this model, all the mole fraction solubilities at different temperatures fit in a single straight line when plotted using eq 4. In this model, y_2 is the mole fraction solubility of the solute in the $scCO_2$; ρ_1 is the density of the $scCO_2$; T and P are the operating temperature and pressure; and α, β, and γ are constants obtained by a multiple linear regression of the experimental solubility data.

$$T \ln(y_2 \cdot P) = \alpha + \beta\rho_1 + \gamma T \quad (4)$$

Data in Table 1 were correlated as a function of the absolute temperature (T) and pressure (P) of the system and the density of the $scCO_2$ (ρ_1) using the model of Mendez−Santiago and Teja. Then, best-fit values of the model parameters ($\alpha = -9203$ K, $\beta = 2.805$ $K \cdot L \cdot g^{-1}$, and $\gamma = 21.74$) for the solubility of TDA in $scCO_2$ are presented in Figure 5 with the line equation of $y = 2.8047x - 9203.6$, $R^2 = 0.9964$.

The line is presented in Figure 4 for TDA, and the experimental data from Table 1 show that solubility values increase with both temperature and pressure of the system. The isothermal increase in solubility with pressure was due to the increase in the density and the associated increase in the solvating power of $scCO_2$. At low pressures, the reduction in solvating power of the $scCO_2$ resulting from a decrease in the density while increasing the temperature isobarically was

Table 1. TDA Solubility in Mole Fraction (y_2), in g_{TDA} per L of Expanded CO_2 Gas (S),[a] and the Density of $scCO_2$[b] at Temperatures of (308, 318, and 328) K and a Pressure Range of (8.0 to 40.0) MPa

	P / MPa	100 y_2	$100S$ / $g_{TDA} \cdot L^{-1}_{CO2}$	$scCO_2$ density / $kg \cdot m^{-3}$
$T = 308$ K	8.0	0.018 ± 0.002	0.33 ± 0.03	419.09
	8.5	0.094 ± 0.008	1.75 ± 0.15	612.12
	9.0	0.161 ± 0.012	3.00 ± 0.20	662.13
	10.0	0.225 ± 0.021	4.17 ± 0.38	712.81
	12.0	0.318 ± 0.036	5.91 ± 0.66	767.07
	15.0	0.375 ± 0.035	6.97 ± 0.65	815.70
	20.0	0.388 ± 0.025	7.22 ± 0.47	865.72
	25.0	0.389 ± 0.033	7.24 ± 0.62	901.23
	30.0	0.400 ± 0.042	7.45 ± 0.78	929.11
	35.0	0.410 ± 0.033	7.63 ± 0.60	952.29
	40.0	0.420 ± 0.038	7.82 ± 0.70	972.26
$T = 318$ K	8.0	0.008 ± 0.001	0.16 ± 0.02	241.05
	8.5	0.011 ± 0.002	0.21 ± 0.02	281.81
	9.0	0.015 ± 0.002	0.29 ± 0.03	337.51
	10.0	0.048 ± 0.006	0.89 ± 0.11	498.25
	12.0	0.180 ± 0.013	3.34 ± 0.24	657.74
	15.0	0.459 ± 0.046	8.54 ± 0.87	741.97
	20.0	0.556 ± 0.050	10.37 ± 0.94	812.69
	25.0	0.612 ± 0.032	11.41 ± 0.59	857.14
	30.0	0.635 ± 0.057	11.84 ± 1.07	890.33
	35.0	0.660 ± 0.066	12.31 ± 1.23	917.12
	40.0	0.672 ± 0.047	12.50 ± 0.90	939.75
$T = 328$ K	8.0	0.011 ± 0.001	0.21 ± 0.01	203.64
	8.5	0.015 ± 0.002	0.27 ± 0.03	227.84
	9.0	0.023 ± 0.004	0.43 ± 0.07	255.55
	10.0	0.036 ± 0.005	0.66 ± 0.07	325.07
	12.0	0.093 ± 0.013	1.72 ± 0.24	504.51
	15.0	0.251 ± 0.031	4.66 ± 0.50	635.50
	20.0	0.482 ± 0.041	8.98 ± 0.77	754.61
	25.0	0.641 ± 0.050	11.96 ± 0.94	810.65
	30.0	0.847 ± 0.077	15.83 ± 1.44	850.22
	35.0	1.094 ± 0.098	20.50 ± 1.84	881.17
	40.0	1.126 ± 0.090	21.10 ± 1.70	906.77

[a] Solubility data used in Figure 3. [b] Taken from http://webbook.nist.gov/chemistry/fluid/.

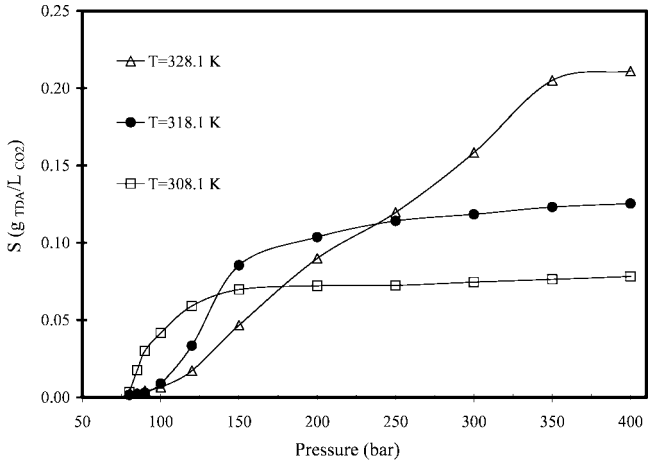

Figure 4. Correlation plots of $\ln(y_2P/P_{ref})$ versus ρ_1/kg · m^{-3} for TDA in the pressure range of (8.0 to 40.0) MPa at temperatures □, 308.1 K; ●, 318.1 K; and △, 328.1 K using the Bartle equation.

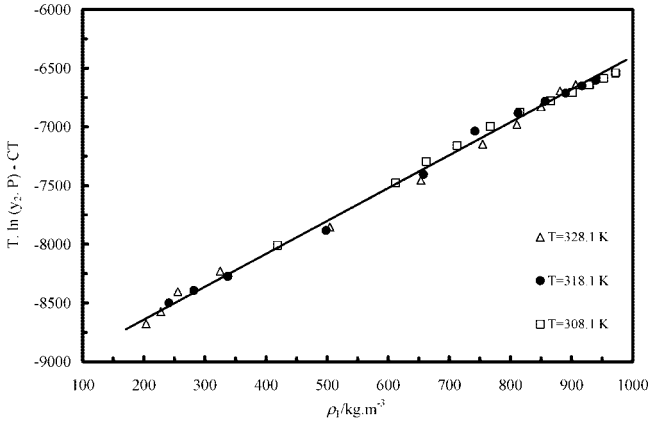

Figure 5. Plots of $T \cdot \ln(y_2 \cdot P) - CT$ versus ρ_1 for TDA in the pressure range of (8.0 to 40.0) MPa for temperatures □, 308.1 K; ●, 318.1 K; and △, 328.1 K using the Mendez−Santiago and Teja model.

partially compensated by an increment in the solute volatility.[28] Two semiempirical equations presented by Chrastil[29] and Mendez−Santiago and Teja are commonly employed to correlate the solid solubility in $scCO_2$, but the results shown in Figure 5 for the liquid TDA solubility at different temperatures indicate that isotherms of (308.1, 318.1, and 328.1) K collapse to a single line and can linearly correlate the data so that α and β are independent of temperature as predicted by the Mendez−Santiago and Teja model. While at these temperatures and pressures, the Chrastil equation did not correlate the solubility data of TDA as well as the Mendez−Santiago and Teja model. For solubility data up to medium pressures of 20.0 MPa, one can apply the Chrastil method, a purely phenomenological model, which is based on some rather physical arguments and gives a linear relation between the logarithm of the solvent density and solubility.

In Table 2, slope, C, intercept, R^2, and AARD (%) are given for the Bartle equation at different temperatures and the pressure range of (8.0 to 40.0) MPa. Because of having better correlation coefficients (R^2) obtained by the Mendez−Santiago and Teja model (Figure 5) in comparison with the Bartle model (Figure 4), we may conclude that our data are better correlated by the Mendez−Santiago and Teja model in the pressure range of (8.0 to 40.0) MPa. Finally, the high solubility of TDA in $scCO_2$ especially at high pressures and temperatures makes the system very attractive for various separation processes listed in the Introduction section.

Table 2. Intercept, Slope *C*, and AARD of the Bartle Equation for TDA at Different Temperatures and in the Pressure Range of (8.0 to 40.0) MPa for the Data Shown in Figure 4

T/K	n^a	*C*	intercept	R^2	AARD^b/%
308	11	0.0085	− 7.68	0.9943	13.63
318	10	0.0088	− 7.19	0.9959	12.86
328	10	0.0084	− 6.27	0.9951	9.07

[a] Number of data points used in the correlation. [b] Average absolute relative deviation.

Conclusions. Solubility of TDA in $scCO_2$ was measured in the pressure range of (8.0 to 40.0) MPa at different temperatures of (308.1, 318.1, and 328.1) K. The data of different temperatures were correlated by the semiempirical Bartle equation and the Mendez−Santiago and Teja model, and the Mendez−Santiago and Teja model was able to better correlate the solubility data. Generally, the solubility of TDA in $scCO_2$ may be considered high, especially at 328.1 K and pressures above 30.0 MPa.

Acknowledgment

Special thanks must go to Mr. Ahmad Rahmanian for his kind assistance in some experiments.

Literature Cited

(1) Yuvaraj, H.; Hwang, H. S.; Jung, Y. S.; Kim, J. H.; Hong, S. S.; Lim, K. T. Dispersion polymerization of styrene in supercritical CO_2 in the presence of non-fluorous random copolymeric stabilizers. *J. Supercrit. Fluids* **2007**, *42*, 351–358.
(2) Kendall, J. L.; Canelas, D. A.; Young, J. L.; Desimone, J. M. Polymerization in supercritical CO_2. *Chem. Rev.* **1999**, *99*, 543–563.
(3) Murga, R.; Sanz, M. T.; Beltran, S.; Cabezas, J. L. Solubility of some phenolic compounds contained in grape seeds, in supercritical CO_2. *J. Supercrit. Fluids* **2002**, *23*, 113–121.
(4) Macnaughton, S. J.; Kikic, I.; Foster, N. R.; Alessi, P.; Cortesi, A.; Colombo, I. Solubility of anti-inflammatory drugs in supercritical CO_2. *J. Chem. Eng. Data* **1996**, *41*, 1083–1086.
(5) Licence, P.; Ke, J.; Sokolova, M.; Ross, S. K.; Poliakoff, M. Chemical reactions in supercritical CO_2: from laboratory to commercial plant. *Green Chem.* **2003**, *5*, 99–104.
(6) Iwao, S.; Abd El-Fatah, S.; Furukawa, K.; Seki, T.; Sasaki, M.; Goto, M. Recovery of palladium from spent catalyst with supercritical CO_2 and chelating agent. *J. Supercrit. Fluids* **2007**, *42*, 200–204.
(7) Meguro, Y.; Iso, S.; Yoshida, Z.; Tomioka, O.; Enokida, Y.; Yamamoto, I. Decontamination of uranium oxides from solidw as tes by supercritical CO_2 leaching method using HNO_3−TBP complex as a reactant. *J. Supercrit. Fluids* **2004**, *31*, 141–147.
(8) Enokida, Y.; Abd El-Fatah, S.; Wai, C. M. Ultrasound-enhanced dissolution of UO_2 in supercritical CO_2 containing a CO_2-philic complexant of tri-n-butylphosphate. *Ind. Eng. Chem. Res.* **2002**, *41*, 2282–2286.
(9) Christov, M.; Dohrn, R. High-pressure fluid phase equilibria: Experimental methods and systems investigated 1994−1999). *Fluid Phase Equilib.* **2002**, *202*, 153–218.
(10) Lucien, F. P.; Foster, N. R. Solubilities of solid mixtures in supercritical CO_2: a review. *J. Supercrit. Fluids* **2000**, *17*, 111–134.
(11) Guigard, S. E.; Stiver, W. H. A density-dependent solute solubility parameter for correlating solubilities in supercritical fluids. *Ind. Eng. Chem. Res.* **1998**, *37*, 3786–3792.
(12) Peng, C. J.; Robinson, D. B. A new two-constant equation of state. *Ind. Eng. Chem. Fundam.* **1976**, *15*, 59–64.
(13) Caplow, M. Kinetics of carbamate formation and breakdown. *J. Am. Chem. Soc.* **1968**, *90*, 6795–6803.
(14) Hampe, E. M.; Rudkevich, D. M. Exploring reversible reactions between CO_2 and amines. *Tetrahedron* **2003**, *59*, 9619–9625.
(15) Dijkstra, Z. J.; Doornbos, A. R.; Weyten, H.; Ernsting, J. M.; Elsevier, C. J.; Keurentjes, J. T. F. Formation of carbamic acid in organic solvents and in supercritical CO_2. *J. Supercrit. Fluids* **2007**, *41*, 109–114.
(16) Selva, M.; Tundo, P.; Perosa, A. The synthesis of alkyl carbamates from primary aliphatic amines and dialkyl carbonates in supercritical CO_2. *Tetrahedron Lett.* **2002**, *43*, 1217–1219.
(17) Li, Z.; Qin, W.; Wang, M.; Huang, Y.; Dai, Y. Equilibrium of extraction of succinic, malic, maleic and fumaric acids with trioctylamine. *Chin. J. Chem. Eng.* **2002**, *10*, 281–285.
(18) Sadaka, M.; Garcia, A. Extraction of shikmik and quinic acids. *Chem. Eng. Commun.* **1999**, *173*, 91–102.

(19) Balcerzak, M.; Wyrzykowska, E. Extraction and preconcentration of platinum and ruthenium using high molecular weight amines prior to simultaneous determination by derivative spectrophotometry. *Analysis* **1999**, *27*, 829–834.

(20) Erkey, C. Supercritical CO_2 extraction of metals from aqueous solutions: a review. *J. Supercrit. Fluids* **2000**, *17*, 187–259.

(21) Yazdi, A. V.; Beckman, E. J. Design, synthesis, and evaluation of novel highly CO_2-soluble chelating agents for removal of metals. *Ind. Eng. Chem. Res.* **1996**, *35*, 3644–3652.

(22) Mekki, S.; Wai, C. M.; Billard, I.; Moutiers, G.; Yen, C. H.; Wang, J. S.; Quadi, A.; Gaillard, C.; Hesemann, P. Cu (II) extraction by supercritical fluid CO_2 from a room temperature ionic liquid using fluorinated β-diketones. *Green Chem.* **2005**, *7*, 421–423.

(23) Ghaziaskar, H. S.; Kaboudvand, M. "Solubility of trioctylamine in supercritical carbon dioxide". *J. Supercrit. Fluids* **2008**, *44*, 148–154.

(24) Bartle, K. D.; Clifford, A. A.; Jafar, S. A. Solubility of solids and liquids of low volatility in supercritical CO_2. *J. Phys. Chem. Ref. Data* **1991**, *120*, 713–757.

(25) Mendez-Santiago, J.; Teja, A. S. The solubility of solids in supercritical fluids. *Fluid Phase Equilib.* **1999**, *158*−*160*, 501–510.

(26) Khimeche, K.; Alessi, P.; Kikic, I.; Dahmani, A. Solubility of diamines in supercritical CO_2; experimental determination and correlation. *J. Supercrit. Fluids* **2007**, *41*, 10–19.

(27) Joung, S. N.; Yoo, K. P. Solubility of disperse anthraquinone and dyes in supercritical CO_2 at 313.15 to 393.15 K and from 10 to 25 MPa. *J. Chem. Eng. Data* **1998**, *43*, 9–12.

(28) Brunner, G.; Gas Extraction. *An Introduction to Fundamentals of Supercritical Fluids and the Application to Separation Processes*; Springer: New York, 1994.

(29) Chrastil, J. Solubility of solids and liquids in supercritical gases. *J. Phys. Chem.* **1982**, *86*, 3016–3021.

Received for review March 7, 2008. Accepted April 24, 2008. The authors are grateful to the IUT research council for their financial support of the work.

JE8001656